encit 2020

ABCM Associação Brasileira de Engenharia e Ciências Mecânicas

18th Brazilian Congress of Thermal Sciences and Engineering
November 16-20, 2020 (Online)

ENC-2020-0533
NUMERICAL INVESTIGATION OF THE ASYMMETRY EFFECTS ON TWO-DIMENSIONAL FLOW AROUND A DECENTRALIZED CIRCULAR CYLINDER CONFINED IN A MICROCHANNEL

Bruno Scaramuzza dos Reis[1]
Vinícius Zacharias Martins[1]
Carolina Palma Naveira-Cotta[1]
Renato Machado Cotta[1,2]
[1] Laboratory of Nano and Microfluidics and Micro-Systems – LabMEMS, Mechanical Eng., Dept. – Federal University of Rio de Janeiro, Rio de Janeiro, RJ, Brazil
[2] General Directorate of Nuclear and Technological Development, DGDNTM, Brazilian Navy, Rio de Janeiro, RJ, Brazil
brunoscaramuzza@poli.ufrj.br
vmartins@poli.ufrj.br
carolina@mecanica.coppe.ufrj.br
cotta@mecanica.coppe.ufrj.br

Manish K. Tiwari
Nanoengineered Systems Laboratory, UCL Mechanical Engineering, University College London, London, WC1E 7JE, UK
m.tiwari@ucl.ac.uk

Abstract. *The study of the flow over confined cylinders in microchannels is important as a method of heat transfer and mixing enhancement at microscales. A numerical investigation on the two-dimensional flow over a circular cylinder asymmetrically confined in a microchannel, based on the finite volume method, is here reported. The work aimed to evaluate the effect on the flow behavior due to the decentralization of the cylinder at blockages up to 0.60. Results for the Strouhal number, mean value of the drag coefficient and root mean square of the lift coefficient are in good agreement with data from the literature. The time-averaged pressure coefficient on the cylinder surface decreases as the cylinder is moved towards the wall, with an intensified effect at lower blockage ratios. The asymmetric confinement of the cylinder with blockage ratios greater than 0.40 causes a suppression of the beating phenomenon and vortex shedding.*

Keywords: *circular cylinder, confinement effects, vortex shedding, pressure coefficient, microchannel*

1. INTRODUCTION

With the increasing application possibilities of different micro mixers, micro reactors and micro heat exchangers in the industry, there is a need to better understand, analyze, and optimize the heat and mass transfer processes that occur in such micro-devices. Recently, a large number of investigations were conducted to analyze the flow around confined cylinders in microchannels (Zovatto and Pedrizzetti (2001), Sahin and Owens (2004), Mettu et al. (2006), Hsieh and Chen (2006), Camarri and Giannetti (2010), Singha and Sinhamahapatra (2010), Griffith et al. (2011), Kanaris et al. (2011), Zhang et al. (2019) and Zhang et al. (2020)) to better understand the physical behavior of the flow regarding heat and mass transfer enhancement at the microscale. In this context, this work aims to numerically study the influence of the two-dimensional flow around a decentralized circular cylinder confined in a microchannel, in order to understand the combined effects of the decentralization and blockage ratios from 0.10 up to 0.60, in the range of Reynolds number from 120 to 400.

The effect of the symmetric lateral confinement on the onset of the vortex shedding was numerically investigated for two-dimensional (2D) flow by Sahin and Owens (2004) through a linear stability analysis, for blockage ratios of 0.1 to 0.9, and Reynolds number from 0 to 280. It was found that the critical Reynolds number decreases as the blockage ratio decreases, approaching the unbounded case. Direct numerical simulations were performed to verify the results and vortex shedding from the cylinder and the channel walls were observed for blockages from 0.50 to 0.90. The numerical simulations enabled to calculate the mean value of the drag coefficient, which decreased with the Reynolds number and increased with the blockage ratio. Besides the drag coefficient, the Strouhal number and the lift coefficient were numerically studied by Singha and Sinhamahapatra (2010) for the 2D flow at blockage ratios from 0.125 to 0.50 and Reynolds number from 45 to 250. The root mean square of the lift coefficient decreased and the Strouhal number increased as the blockage ratio varied from 0.125 to 0.50. For blockage ratios greater than 0.30, the Strouhal number was

independent of the Reynolds number, indicating that the vortices grow up to a certain level before the shedding occurs. The influence of the lateral confinement on the development of 3D instabilities in macroscale flow around a circular cylinder was investigated by Camarri and Giannetti (2010) through a theoretical linear stability analysis, and Kanaris et al. (2011) with direct numerical simulations. The 3D instabilities showed similar patterns than the ones observed at the unconfined case with a delay on the onset of the mode A instability. It was observed that the walls are responsible for an earlier breakdown of these instabilities. The influence of the symmetric confinement on the shedding frequency was numerically studied by Griffith et al. (2011) for 2D flow with blockage ratios from 0.10 to 0.90 and Reynolds number from 50 to 300, observing a decrease on the Strouhal number as the blockage ratio increases from 0.80 to 0.90. It was found that for blockage ratios greater than 0.50, a second and lower frequency appears in the lift and drag coefficients due to the vortices shed off from the channel walls, resulting in the beating phenomenon that decays over a very long time-scale. For the blockage of 0.50 this phenomenon began at a Reynolds of 285, approximately. The 3D flow over a symmetrically confined circular cylinder inside a microchannel was investigated by Zhang et al. (2019) with a new experimental system capable of fully resolving the high frequencies of the microscale flow. It was observed that the vertical confinement has a stronger effect on the suppression of the vortex shedding than the lateral confinement. Regarding the shedding frequency, it was practically independent of the vertical confinement, but increases as the blockage ratio is increased.

The asymmetric confinement of a circular cylinder was investigated by Zovatto and Pedrizzetti (2001), Mettu et al. (2006), Hsieh and Chen (2006) and Zhang et al. (2020). As the cylinder moves towards one of the walls the vortex shedding is suppressed, similarly to the cases of flow over a cylinder near a plane boundary studied by Lei et al. (2000) and Rao et al. (2013). Zovatto and Pedrizzetti (2001), with a constant blockage ratio of 0.20, and Mettu et al. (2006), with blockages varying from 0.10 to 0.40, numerically investigated the flow around a decentralized cylinder inside a channel. The Strouhal number and the mean value of the drag coefficient decreased as the cylinder approaches one of the walls, excepting the cases where the gap between the cylinder and the wall is so small that the interaction between the viscous boundary layers increases the drag coefficient. The mean value of the lift coefficient changed from positive to negative values according to the proximity to the wall due to the variation of the pressure on the cylinder surface. Hsieh and Chen (2006) numerically studied the steady state 2D flow for blockages from 0.10 to 0.50 and Reynolds number in the range of 50 to 200. The recirculation region attached to the cylinder decreases its size as the cylinder approaches the wall. For small gaps it changes to a recirculation region attached to the wall, similarly to the case with an obstacle attached to the wall. A 3D experimental investigation was performed by Zhang et al. (2020) to evaluate the effect of the decentralization of a circular cylinder on the mixing of two flows.

With the miniaturization of electronic components and chemical reactors, the placement of pins inside microchannels has been extensively studied due to the desirable heat transfer and mixing enhancement at these lower Reynolds numbers at microscale flows. The importance of the circular cylinders on the heat transfer enhancement was demonstrated by Renfer et al. (2013) for micro heat sinks populated with micropin fins integrated with electronic chip stacks. With respect to the mixing enhancement, Santana et al. (2015) demonstrated the effectiveness of using micropin fins in biodiesel synthesis with micro reactors, with a high oil conversion and low residence time.

From the above review, it is clear that the flow around an asymmetrically confined circular cylinder has been studied in a few investigations. Nonetheless, to the best of our knowledge, there is no published investigation on the decentralized circular cylinder confined in a microchannel with blockage ratios greater than 0.50 and there is no study of the pressure on the surface of the cylinder for the confined circular cylinder in the range of Reynolds from 120 to 400. In light of the above considerations, the aim of this work is to numerically investigate the effect of the asymmetric confinement on the 2D flow around a circular cylinder with blockage ratios from 0.10 up to 0.60, and Reynolds number ranging from 120 to 400.

2. ANALYSIS

The problem formulation and solution methodology employed in this study are described next, detailing the governing equations, the computational domain and mesh, as well as the mesh independence analysis.

2.1 Mathematical Model

The governing equations for the transient 2D incompressible viscous flow in the absence of external forces and gravity, and considering the laminar regime, are the continuity and momentum conservation, written as:

$$\nabla \cdot \boldsymbol{U} = 0 \tag{1}$$

$$\frac{\partial \boldsymbol{U}}{\partial t} + \boldsymbol{U} \cdot \nabla \boldsymbol{U} = -\frac{1}{\rho}\nabla p + \nu \nabla^2 \boldsymbol{U} \tag{2}$$

where ρ is the fluid density, p is the pressure, ν is the kinematic viscosity and $\boldsymbol{U}$ is the velocity vector with components U_x and U_y for two-dimensional flow. The physical properties of water at the constant temperature of 293 K were taken

for the calculations, with the values for the fluid density ρ and kinematic viscosity ν equal to 1000 kg/m^3 and 10^{-6} m^2/s, respectively.

The discretization of the continuity and momentum conservation equations were performed using the finite volume method with the commercial software ANSYS Fluent 2019 R2. The mean value of the drag coefficient (C_{Dm}), the root mean square of the lift coefficient (C_{Lrms}), the Strouhal number (St), the pressure coefficient on the cylinder surface (C_p) and the pressure drop were analyzed.

2.2 Computational Procedure

The domain of the problem is illustrated in Fig. 1, where D represents the diameter of the cylinder, W is the width of the channel, Δy is the distance between the cylinder and one of the lateral walls, the distance between the cylinder center and the inlet and outlet of the channel are represented by L_i and L_o, respectively. U_{max} is the maximum velocity of the fluid at the inlet. The lengths L_i and L_o are equal to 12D and 35D, following the same proportions presented by Alfieri *et al.* (2013). The width of the channel W is constant and equal to 10^{-3} m, and the diameter of the cylinder changed with the blockage ratio, from a minimum value of 1x10^{-4} m (blockage ratio of 0.10) to the maximum of 6x10^{-4} m (blockage ratio of 0.60).

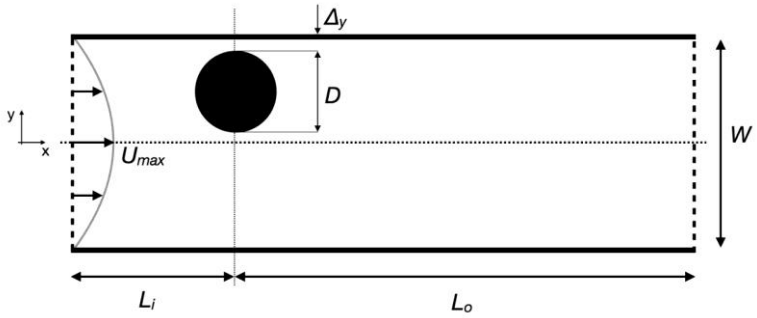

Figure 1. Schematic representation of the computational domain.

A no-slip condition ($U_x = U_y = 0$) was imposed on the walls of the channel and at the cylinder surface, a zero-gauge pressure was set at the outlet of the channel and at the inlet a fully developed velocity profile, defined in Eq. (3) and with $U_y = 0$, was used.

$$U_x(y) = U_{max}\left[1 - 4\left(\frac{y}{H}\right)^2\right] \tag{3}$$

The geometric parameters of the problem are the blockage ratio β and gap ratio γ. The blockage ratio is the ratio of cylinder diameter to channel width, while the gap ratio represents the proximity of the cylinder to the wall, and are respectively given by:

$$\beta = \frac{D}{W} \tag{4}$$

$$\gamma = \frac{\Delta y}{\left(\frac{W}{2} - \frac{D}{2}\right)} \tag{5}$$

The maximum velocity of the fluid at the inlet U_{max} and the diameter D of the cylinder were taken as the characteristic parameters of the flow. Due to the range of Reynolds number analyzed, and in accordance with the study of Martins (2018), the simulation was performed using the laminar flow regime.

The blockage ratio in this study varied from 0.10 to 0.60 and, for each blockage ratio, three distinct gap ratios (0.25, 0.50 and 0.75) and four Reynolds numbers (120, 200, 300 and 400) were analyzed, totaling 72 simulated cases. Before proceeding to the physical and parametric analyses, a convergence investigation was undertaken. The analysis of the spatial mesh was performed at the steady state regime, resulting in a relative deviation of less than 0.03% for all evaluated quantities: the mean values of the drag and lift coefficients, and the pressure coefficient on the stagnation point at the cylinder surface. Once the spatial convergence was achieved the temporal discretization was analyzed with a semi-implicit method, resulting in the final higher relative deviation of 1.6% for the root mean square of the lift coefficient.

Figure 2 illustrates the spatial mesh used in this study. The final spatial mesh was not represented here due to the inconvenience generated by the great number of elements. As it can be seen, the mesh is refined near the walls of the channel and closely around the cylinder surface.

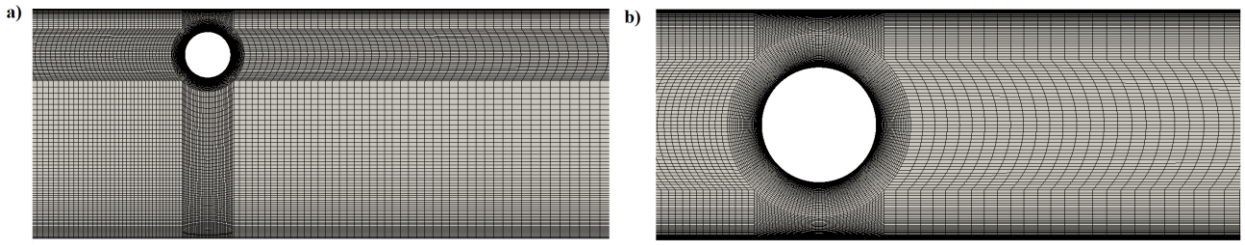

Figure 2. Schematic representation of the spatial mesh for the case with (a) blockage ratio of 0.20 and gap ratio of 0.25 and (b) blockage ratio of 0.50 and gap ratio of 1.0.

3. RESULTS AND DISCUSSION

To analyze the relationship between the gap ratio and Reynolds number different blockage ratios of 0.10, 0.20, 0.30, 0.40, 0.5 and 0.60 were simulated. For each blockage, the simulated gap ratios were 0.25, 0.50 and 0.75, and for each of them four different Reynolds numbers: 120, 200, 300 and 400, summering up 72 simulated cases.

As a first verification of the simulation here implemented, the results of the mean drag coefficient and Strouhal number for the case with blockage ratio 0.10 were compared with previously published results by Mettu et al. (2006). In their work, Mettu et al. (2006) numerically solved the governing flow and energy equations for blockage ratios from 0.10 to 0.40 and Reynolds from 10 to 500. The present results are in overall good agreement with the results from Mettu et al. (2006), with a maximum relative error of less than 7%, as it can be seen in Figs. 3(a)-(b) for the blockage ratio of 0.10. Due to the greater maximum deviation at the case "β 0.10 - γ 0.75", numerical simulations were performed with a finer spatial mesh, showing no significant alteration. In addition to the finer spatial mesh, a couple of cases without vortex shedding were evaluated considering steady state, reducing the maximum relative deviation.

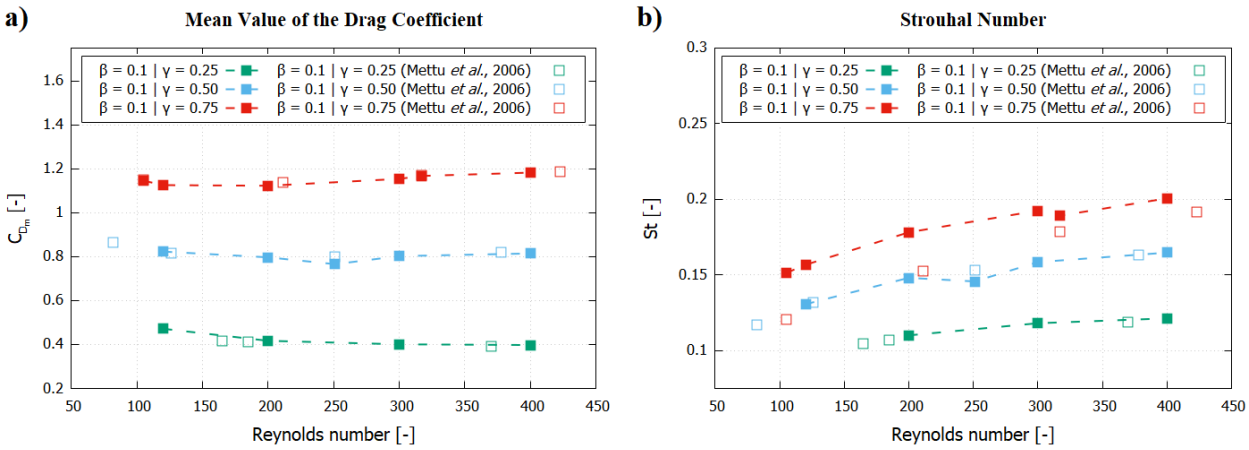

Figure 3. Comparison between the present results and the values of Mettu et al. (2006) for the (a) mean value of the drag coefficient and (b) the Strouhal number for the blockage ratio of 0.10.

In order to investigate the effects of the asymmetrical displacement of the cylinder at higher blockage ratios on the mean value of the drag coefficient, Fig. 4(a) shows the results for the blockages of 0.50 and 0.60. It can be seen that the drag coefficient decreases with the Reynolds number for a fixed blockage and gap ratios, showing the same behavior as with the unconfined case at the range of Reynolds number evaluated. For a fixed Reynolds number, the drag coefficient greatly increases with the blockage ratio, as the channel becomes more obstructed with the cylinder. The results show a minor dependence of the drag coefficient on the gap ratio for fixed blockage ratios of 0.50 and 0.60. At blockage ratios greater than 0.40 the decentralization of the cylinder in the channel has a strong influence on the suppression of the vortex shedding, with vortex shedding appearing only for the cases "β 0.50 - γ 0.75 - Re 200", "β 0.50 - γ 0.75 - Re 300", "β 0.50 - γ 0.75 - Re 400" and "β 0.50 - γ 0.50 - Re 400". Figure 4(b) presents the relationship between the Strouhal and Reynolds numbers for the blockage ratio of 0.50 and gap ratios of 0.75 and 0.50, decreasing its value with increasing Reynolds number. It is possible to observe a slight decrease on the Strouhal number as the cylinder changes from a centralized to a decentralized position in the channel, indicating that as the blockage ratio increases, the gap ratio has a reduced effect on the Strouhal number.

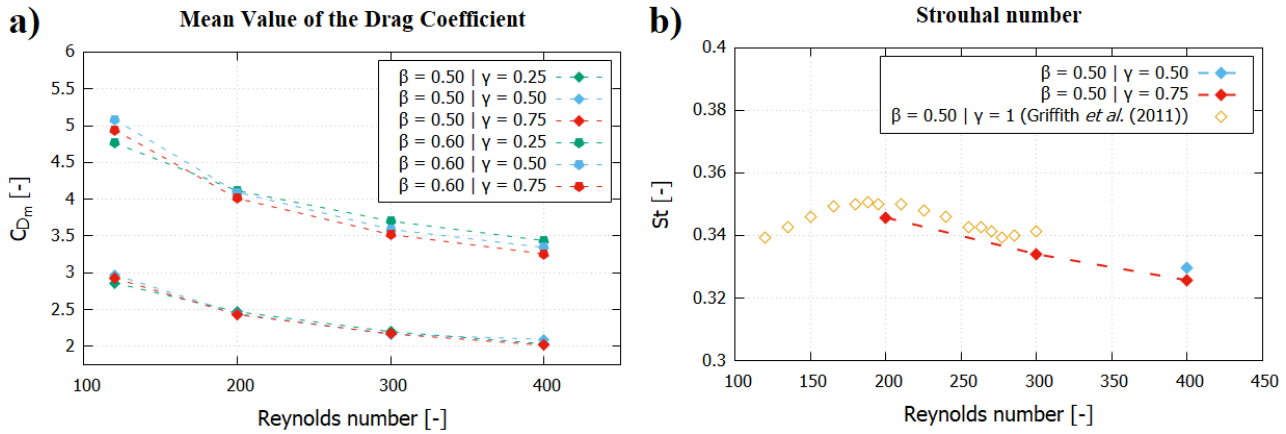

Figure 4. Variation with Reynolds number for the (a) mean value of the drag coefficient and (b) the Strouhal number, for blockage ratios of 0.50 and 0.60 (due to the suppression of vortex shedding at the blockage ratio of 0.60, the Strouhal number only presents the results for the blockage ratio of 0.50).

At the blockage ratio of 0.60 the asymmetrical position of the circular cylinder in the channel suppressed the vortex shedding for the range of Reynolds number evaluated, giving place to multiple recirculation regions attached to the walls downstream from the cylinder. Figures 5(a)-(c) show the velocity plots of the cases with blockage ratio equal to 0.60 and gap ratio from 0.75 to 0.25. In the three figures, the velocity ranges from 0 (blue) to 1.4 m/s (red). As the cylinder moves towards the wall, the number of recirculation regions decreases and their sizes increase, with a similar behavior as for the case with an obstacle attached to the wall at the gap ratio of 0.25.

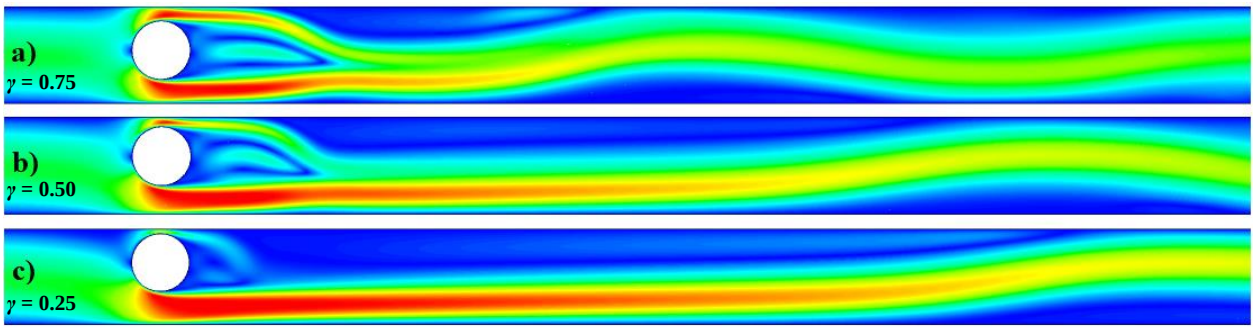

Figure 5. Velocity contours for the case with blockage ratio of 0.60, Reynolds number of 400 and gap ratio of (a) 0.75, (b) 0.50 and (c) 0.25. For all three cases, the velocity varies from 0 (blue) to 1.4 m/s (red).

For the cases “β 0.50 - γ 0.75 - Re 300” and “β 0.50 - γ 0.75 - Re 400” it was possible to identify the beating phenomenon. This is in agreement with the results of Griffith et al. (2011) and Martins (2018) that, at Reynolds number higher than 280, this phenomenon occurs due to the greater interaction between the vortices shed from the cylinder and the shear layers of the channel walls, leading to a regular detachment of the shear layers from the wall, which merges with the vortices downstream the cylinder. However, for the case “β 0.50 - γ 0.75 - Re 400” the decentralization of the cylinder generates a recirculation region attached to the wall near the cylinder, which interacts with the vortices shed from the cylinder and the stretched shear layers of the channel wall, strongly affecting the beating phenomenon, as it can be seen in Figs. 6(a)-(h) with the variation of the lift and drag coefficients through time and the spanwise vorticity contours at six distinct instants of time.

It can be observed that the vortex shedding occurs farther away from the cylinder (Fig. 6(c) and (h)), leading to smaller amplitudes on the lift and drag coefficients. At this regime, the vortices are stretched due to the presence of the shear layers of the wall and a single recirculation region downstream the cylinder at the upper wall, contributing to the dissipation of the vortex energy. Since the vortices and the wall shear layer merge together, there is no regular vortex street downstream the cylinder. As the wake moves closer to the cylinder, the vortices are no longer being stretched and can develop a regular and stronger vortex, with the presence of an evident reverse von Kármán street downstream the cylinder (Fig. 6(e) and (g)). As the vortices are generated closer to the cylinder, the interaction with the walls is stronger, since the vortices are pushed to the wall at the opposite side. This interaction breaks the single recirculation region into multiple small recirculation regions that move along with the vortices. Finally, these small regions near the cylinder grow (Fig. 6(f)) until a size that it can assist the wall shear layers through the stretching process and, consequently, the dissipation of the vortex street.

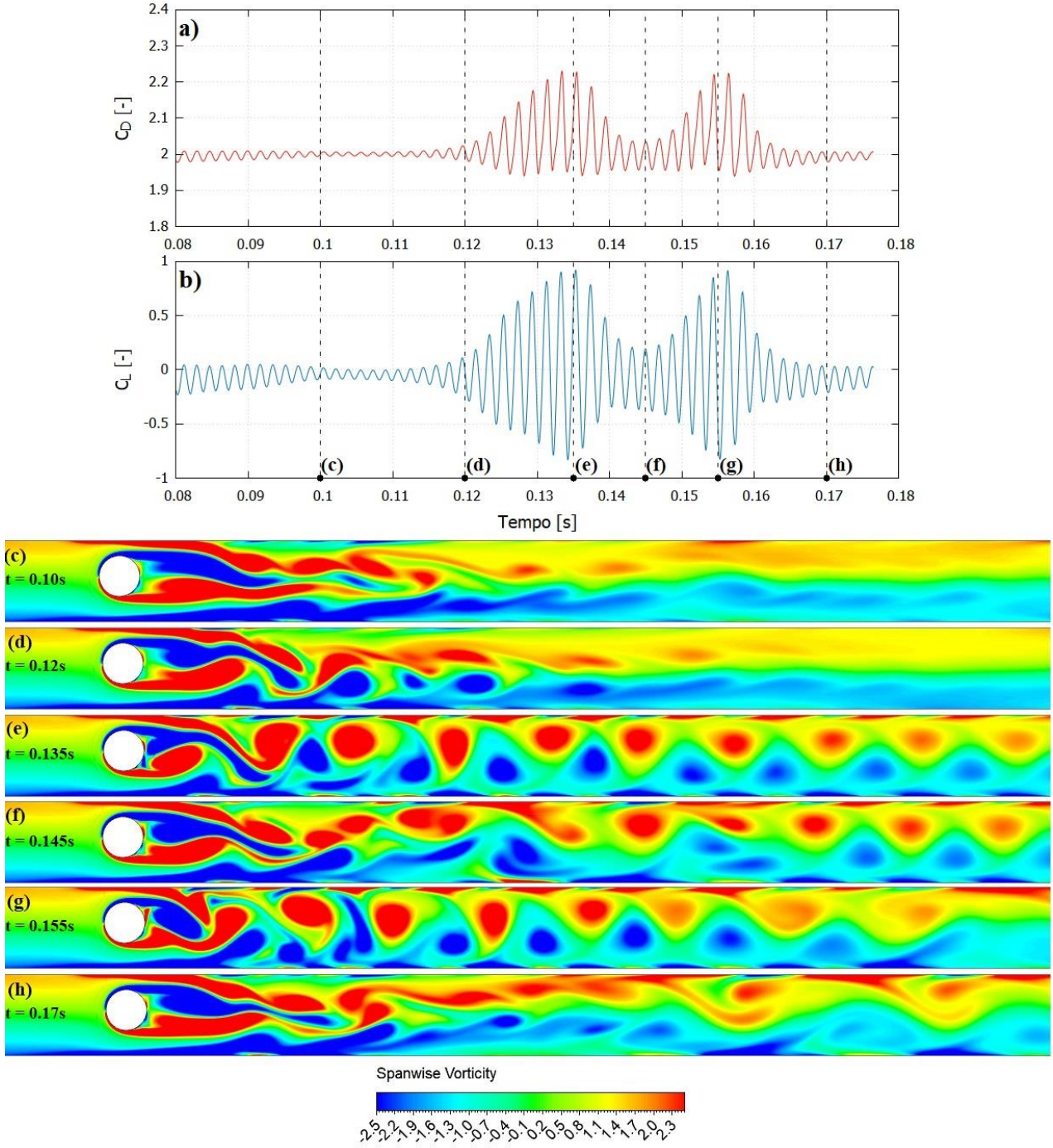

Figure 6. Results of the case "β 0.50 - γ 0.75 - Re 400" for the (a) drag coefficient, (b) lift coefficient and (c-h) the contours of the spanwise vorticity ($\boldsymbol{\omega_z}$) at six instants of time.

In order to investigate the pressure drop along the channel for blockage ratios from 0.10 up to 0.60, Figs. 7(a)-(f) present this parameter in nondimensional form as a friction factor *f*, defined as:

$$f = \frac{\Delta P}{0.5\rho U_{\max}^2} \frac{D}{(L_i + L_o)} \tag{6}$$

where ΔP is the pressure drop along the channel, D is the cylinder diameter, ρ is the fluid density, U_{max} is the maximum velocity of the fluid at the inlet and $L_i + L_o$ is the total length of the channel.

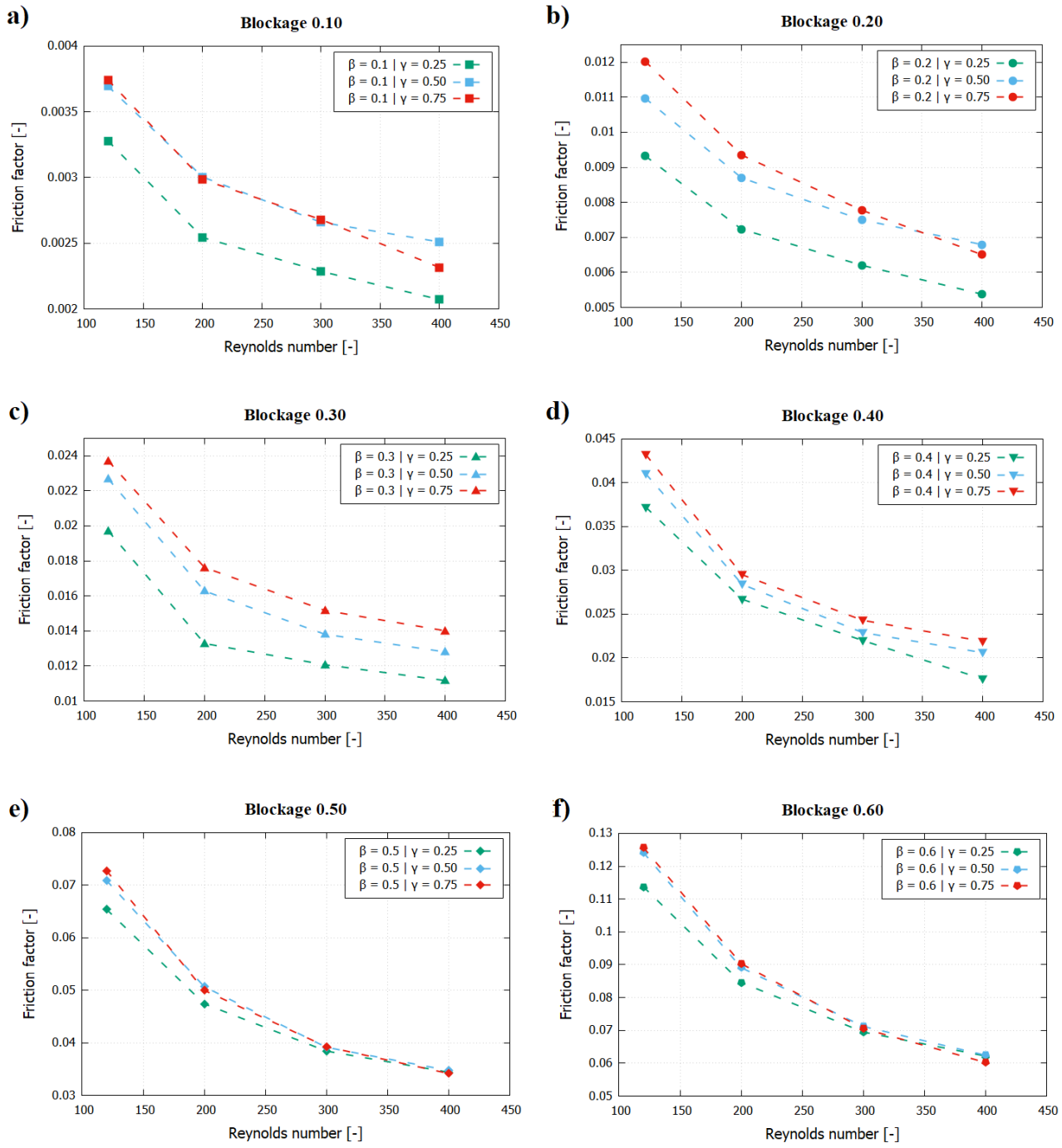

Figure 7. Behavior of the friction factor *f* in terms of the Reynolds number for the blockage ratios of (a) 0.10, (b) 0.20, (c) 0.30, (d) 0.40, (e) 0.50 and (f) 0.60.

The friction factor shows a similar behavior as the mean value of the drag coefficient, decreasing its value as the Reynolds number is increased for fixed blockage and gap ratios, and drastically increases as the blockage ratio is increased from 0.10 to 0.60, with a friction factor at the blockage ratio of 0.60 more than 26 times the friction factor at the blockage ratio of 0.10. In addition, the friction factor decreases as the cylinder approaches the wall, with this effect being stronger for lower blockages. Besides the vortex suppression at higher blockage ratios, which decreases the mixing and heat transfer enhancement aimed with the insertion of a pin in the microchannel, the significant increase on the friction factor suggests that greater blockage ratios are undesirable for the enhancement of the mixing process in microchannels.

Regarding the effect of the gap ratio on the time-averaged pressure coefficient, Figs. 8(a)-(f) show its behavior for different blockage ratios with a fixed Reynolds number of 300. As the cylinder moves towards the wall, the distribution of the time-averaged pressure coefficient on the cylinder surface shows an increasing asymmetry, and the pressure coefficient at the stagnation point decreases, with its location moving in the opposite direction of the wall. As the pressure at the stagnation point decreases, the pressure on the opposite side, the base of the cylinder, increases for blockages up to

0.30. At higher blockages, the cylinder occupies a larger area of the channel, leading to a smaller variation on the velocities as the cylinder approaches the wall, explaining the lower variation on the pressure coefficient at higher blockage ratios.

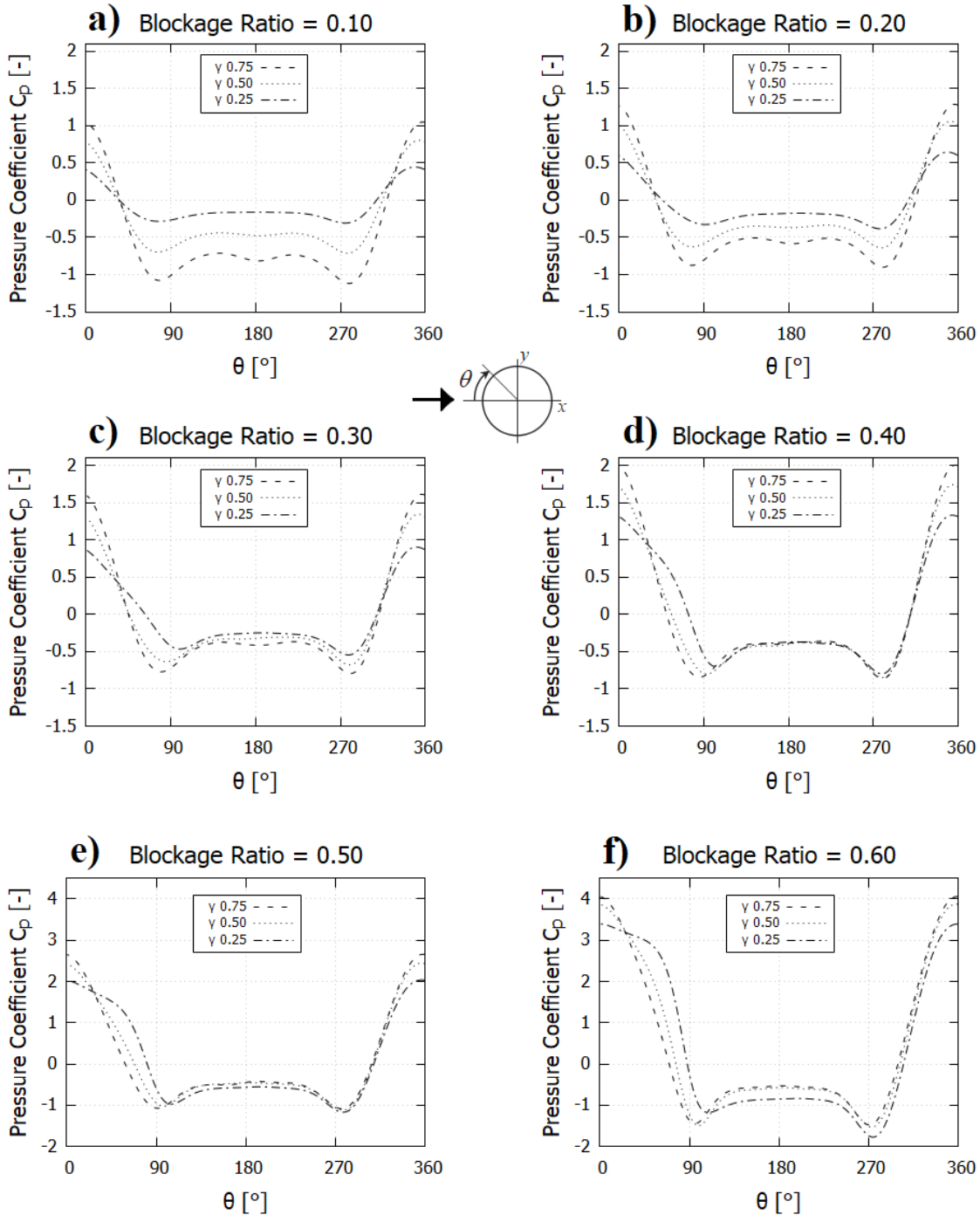

Figure 8. Behavior of the pressure coefficient over the cylinder surface at *Re* = 300 and for blockage ratios of (a) 0.10, (b) 0.20, (c) 0.30, (d) 0.40, (e) 0.50 and (f) 0.60.

Despite the smaller variations, the asymmetric distribution of the pressure becomes more evident in the range of $0^o \leq \theta \leq 90^o$ as the blockage is increased, which occurs due to the larger difference on the velocities on the upper and lower part of the cylinder.

In view of the time variation of the root mean square of the lift coefficient caused by the beating effect, this parameter is presented in Figs. 9(a)-(d) only for the blockage ratio from 0.10 up to 0.40 as it remains constant through time. The C_{Lrms} increases with increasing Reynolds number and drastically decreases as the cylinder moves towards the channel wall, with the proximity of the wall limiting the amplitude of the oscillation of the flow around the cylinder.

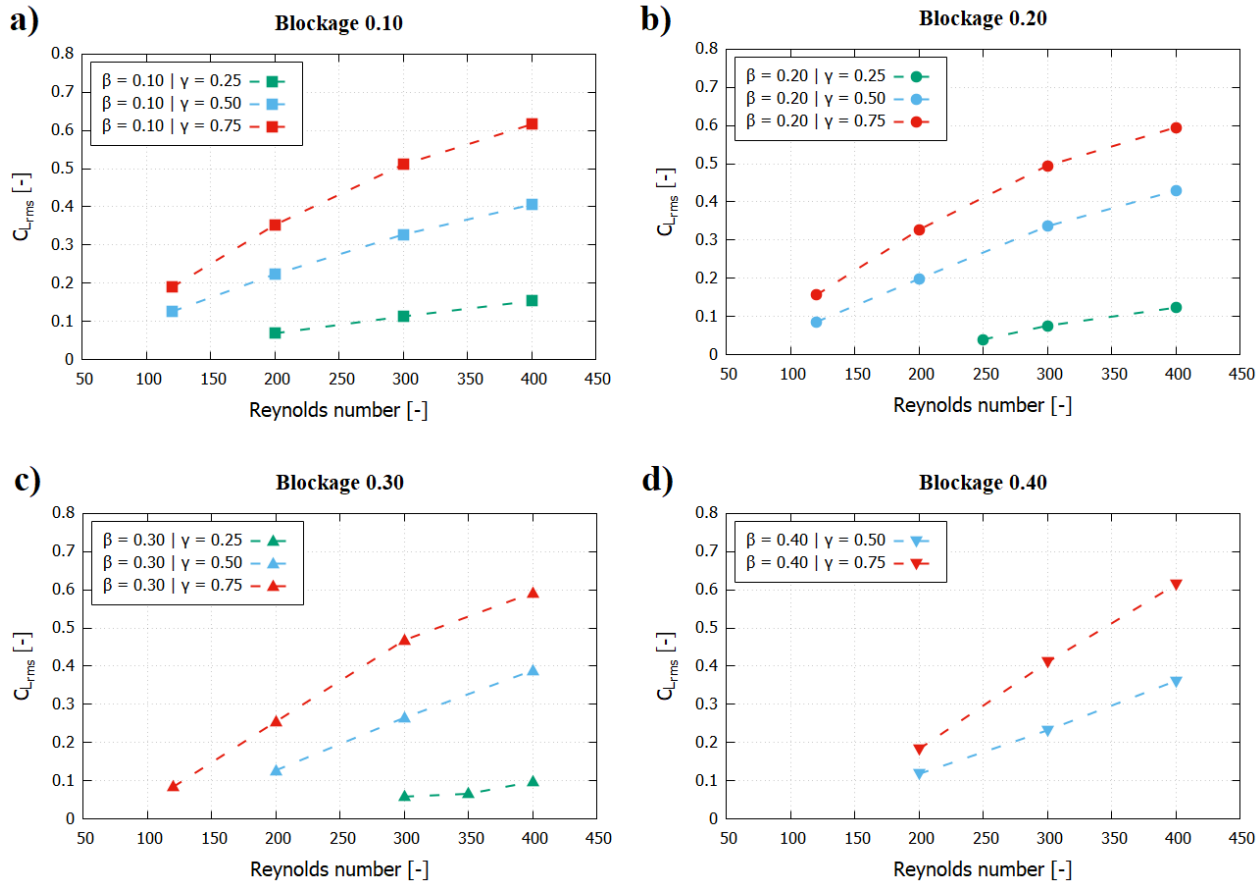

Figure 9. Behavior of the root mean square of the lift coefficient (C_{Lrms}) in terms of the Reynolds number for the blockage ratios of (a) 0.10, (b) 0.20, (c) 0.30 and (d) 0.40.

4. CONCLUSIONS

In this work, the two-dimensional flow around a circular cylinder asymmetrically confined in a microchannel was numerically studied for blockage ratios from 0.10 up to 0.60. It was found that the decentralization of the cylinder strongly affects the flow parameters for lower blockage ratios, decreasing the root mean square of the lift coefficient, the mean value of the drag coefficient and the friction factor for a fixed Reynolds number. As the cylinder diameter increases, the proximity to the wall showed low influence on the flow parameters due to the greater area occupied by the cylinder in the channel. For blockage ratios greater than 0.50 the decentralization had an important effect on the suppression of the vortex shedding and to the multiple recirculation regions that appear downstream of the cylinder. The interaction between the wall shear layers and the vortices was carefully examined in the beating phenomenon for the case with blockage ratio of 0.50, gap ratio of 0.75 and Reynolds number of 400. Regarding the pressure coefficient on the cylinder surface, it was found that the proximity to the wall changes to an asymmetric distribution of the pressure on the cylinder surface, showing a stronger influence at lower blockage ratios. It was also found that the low blockage ratio is responsible for a lower critical Reynolds number and the proximity to the wall decreases the pressure drop. With this in mind, this study suggests that obstacles with low blockage ratios and nearer tp the channel wall could enhance the mixing process without a prohibitive increase in the pressure drop along the channel.

5. ACKNOWLEDGEMENTS

The authors are grateful for the partial financial support provided by the Brazilian funding agencies CNPq, FAPERJ, and CAPES.

6. REFERENCES

Alfieri, F., Tiwari, M.K., Renfer, A., Brunschwiler, T., Michel, B., and Poulikakos, D., 2013. "Computational modeling of vortex shedding in water cooling of 3D integrated electronics". *International Journal of Heat & Fluid Flow*, Vol. 44, pp. 745–755.

Camarri, S. and Giannetti, F., 2010. "Effect of confinement on three-dimensional stability in the wake of a circular cylinder", *Journal of Fluid Mechanics*, Vol. 642, pp. 477-487.

Griffith, M.D., Leontini, J., Thompson, M.C., and Hourigan, K., 2011. "Vortex shedding and three-dimensional behaviour of flow past a cylinder confined in a channel". *Journal of Fluids and Structures*, Vol. 27, pp. 855–860.

Hsieh, T.C., and Chen, J.H., 2006. "Emergence of attached recirculating eddy for flow around a circular cylinder asymmetrically placed in a channel". *Journal of Marine Science and Technology*, Vol. 14, No. 3, pp. 147–154.

Kanaris, N., Grigoriadis, D., and Kassinos, S., 2011. "Three dimensional flow around a circular cylinder confined in a plane channel". *Physics of Fluids*, Vol. 23, 064106.

Lei, C., Cheng, L., Armfield, S. W., and Kavanagh, K., 2000. "Vortex shedding suppression for flow over a circular cylinder near a plane boundary". *Ocean Engineering*, Vol. 27, pp. 1109-1127.

Martins, V.Z., 2018. *Análise Numérica do Escoamento ao Redor de Cilindros Circulares Confinados em Microcanais*. MSc thesis, Universidade Federal do Rio de Janeiro, Rio de Janeiro, Brasil.

Mettu, S., Verma, N., and Chhabra, R.P., 2006. "Momentum and heat transfer from an asymmetrically confined circular cylinder in a plane channel". *Heat and Mass Transfer*, Vol. 42, pp. 1037-1048.

Rao, A., Thompson, M. C., Leweke, T., and Hourigan, K., 2013. "The flow past a circular cylinder translating at different heights above a wall". *Journal of Fluids and Structures*, Vol. 42, pp. 9-21.

Renfer, A., Tiwari, M. K., Tiwari, R., Alfieri, F., Brunschwiler, T., Michel, B., and Poulikakos, D., 2013. "Microvortex-enhanced heat transfer in 3D-integrated liquid cooling of electronic chip stacks". *International Journal of Heat and Mass Transfer*, Vol. 65, pp. 33-43.

Santana, H. S., Júnior, J. L. S., and Taranto, O. P., 2015. "Numerical simulations of biodiesel synthesis in microchannels with circular obstructions". *Chemical Engineering and Processing: Process Intensification*, Vol. 98, pp. 137-146.

Sahin, M., and Owens, R.G., 2004. "A numerical investigation of wall effects up to high blockage ratios on two-dimensional flow past a confined circular cylinder". *Physics of Fluids*, Vol. 16, No. 1, pp. 1305–1320.

Singha, S., and Sinhamahapatra, K.P., 2010. "Flow past a circular cylinder between parallel walls at low Reynolds numbers". *Ocean Engineering*, Vol. 37, pp. 757–769.

Zhang, S., Cagney, N., Balabani, S., Naveira-Cotta, C. P., and Tiwari, M. K., 2019. "Probing vortex-shedding at high frequencies in flows past confined microfluidic cylinders using high-speed microscale particle image velocimetry". *Physics of Fluids*, Vol. 31, 102001.

Zhang, S., Cagney, N., Lacassagne, T., Balabani, S., Naveira-Cotta, C. P., and Tiwari, M. K., 2020. "Mixing in flows past confined microfluidic cylinders: Effects of pin and fluid interface offsetting". *Chemical Engineering Journal*, Vol. 397, 125358.

Zovatto, L., and Pedrizzetti, G., 2001. "Flow about a circular cylinder between parallel walls". *Journal of Fluid Mechanics*, Vol. 440, pp. 1–25.

7. RESPONSIBILITY NOTICE

The authors are the only responsible for the printed material included in this paper.